AD-A187 250 EXPERIMENTAL RESEARCH ON SWEPT SHOCK WAVE/BOUNDARY LAYER INTERACTIONS..(U) PENNSYLVANIA STATE UNIV UNIVERSITY PARK DEPT OF MECHANICAL EN.. G S SETTLES

1/1

UNCLASSIFIED JUN 87 PSU/ME-R-86/87-0034 AFOSR-TR-87-1453 F/G 20/4 NL

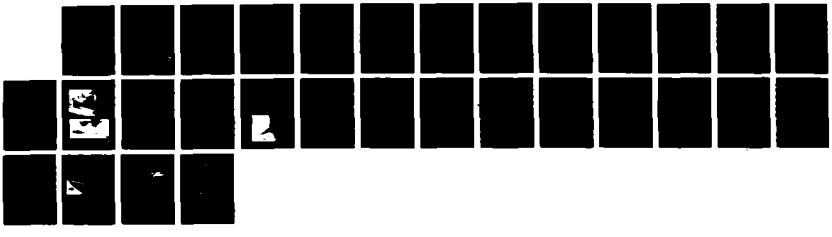

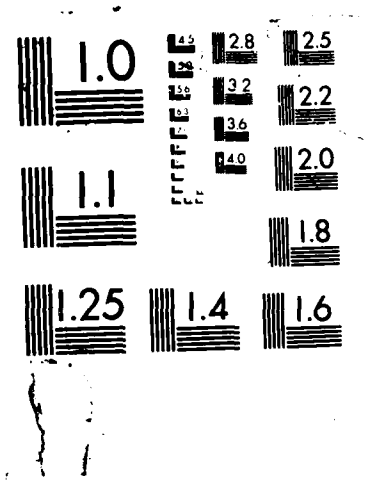
1.0
1.1
1.25
1.4
1.6
2.8
3.2
3.6
4.0
2.5
2.2
2.0
1.8

AFOSR-TR- 87-1453

Department of Mechanical Engineering
Pennsylvania State University
University Park, PA 16802

Report PSU-ME-R-86/87-0034

Experimental Research on Swept Shock Wave/Boundary Layer Interactions

Gary S. Settles

Interim Technical Report for the Period 1 April 1986 to 31 March 1987
on Grant AFOSR-86-0082

submitted to:

Dr. James D. Wilson, Program Manager
US Air Force Office of Scientific Research
Bldg. 410, Bolling AFB, DC 20332-6448

June 1987

PENNSTATE

UNCLASSIFIED
SECURITY CLASSIFICATION OF THIS PAGE

ADA187250

REPORT DOCUMENTATION PAGE

1a. REPORT SECURITY CLASSIFICATION: Unclassified	1b. RESTRICTIVE MARKINGS
2a. SECURITY CLASSIFICATION AUTHORITY	3. DISTRIBUTION / AVAILABILITY OF REPORT: Approved for Public Release; Distribution Unlimited
2b. DECLASSIFICATION / DOWNGRADING SCHEDULE	
4. PERFORMING ORGANIZATION REPORT NUMBER(S): PSU-ME-R-86/87-0034	5. MONITORING ORGANIZATION REPORT NUMBER(S): AFOSR-TR- 87-1453
6a. NAME OF PERFORMING ORGANIZATION: Dept. of Mechanical Engrg., Penn State University; 6b. OFFICE SYMBOL (If applicable)	7a. NAME OF MONITORING ORGANIZATION: Air Force Office of Scientific Research
6c. ADDRESS (City, State, and ZIP Code): University Park, PA 16802	7b. ADDRESS (City, State, and ZIP Code): Building 410, Bolling AFB, Washington, DC 20332
8a. NAME OF FUNDING / SPONSORING ORGANIZATION: Air Force Office of Sci. Res.; 8b. OFFICE SYMBOL (If applicable): AFOSR/NA	9. PROCUREMENT INSTRUMENT IDENTIFICATION NUMBER: AFOSR-86-0082
8c. ADDRESS (City, State, and ZIP Code): Building 410, Bolling AFB, Washington, DC 20332	10. SOURCE OF FUNDING NUMBERS: PROGRAM ELEMENT NO. 61102F; PROJECT NO. 2307; TASK NO. A1; WORK UNIT ACCESSION NO.

11. TITLE (Include Security Classification)
Experimental Research on Swept Shock Wave/Boundary Layer Interactions

12. PERSONAL AUTHOR(S)
Gary S. Settles

13a. TYPE OF REPORT	13b. TIME COVERED	14. DATE OF REPORT (Year, Month, Day)	15. PAGE COUNT
Annual TR	FROM 86/4/1 TO 87/3/31	87/6/26	28

16. SUPPLEMENTARY NOTATION

17. COSATI CODES			18. SUBJECT TERMS (Continue on reverse if necessary and identify by block number)
FIELD	GROUP	SUB-GROUP	High-Speed Flows; Viscous-Inviscid Interactions; Shock-Boundary Layer Interactions; Supersonic Flow, Experiments; Flow Visualization; Fluid Dynamics; Flow Separation

19. ABSTRACT (Continue on reverse if necessary and identify by block number)

The first year of an experimental study of swept shock wave interactions with turbulent boundary layers is reported. Experiments were carried out to assess Mach number effects on interactions due to generic fin and swept compression corner geometries. An extensive set of fin interaction experiments was carried out at constant Reynolds number over the Mach number range of 2.5 to 4.0. Data thus far consist of surface flow visualization photographs and laser light-screen visualizations of flowfield structure. Additional experiments were conducted to assess the possibility that experimental data of this type might depend on the wind tunnel facility in which the experiments were performed. That was not found to be the case. The results of the parametric Mach number study revealed that Mach number effects over the range considered are essentially inviscid. These were accounted for simply by referencing measured quantities to the freestream Mach angle. The interaction growth with increasing shock strength was found to be nonlinear, contrary to previous results. Initial results from swept compression corner experiments are also reported. Finally, second-year research plans are discussed

20. DISTRIBUTION / AVAILABILITY OF ABSTRACT: ☐ UNCLASSIFIED/UNLIMITED ☒ SAME AS RPT ☐ DTIC USERS	21. ABSTRACT SECURITY CLASSIFICATION: Unclassified
22a. NAME OF RESPONSIBLE INDIVIDUAL: DR JAMES WILSON	22b. TELEPHONE (Include Area Code): 202-767-4935; 22c. OFFICE SYMBOL: NA

DD FORM 1473, 84 MAR 83 APR edition may be used until exhausted. All other editions are obsolete.

SECURITY CLASSIFICATION OF THIS PAGE
UNCLASSIFIED

Table of Contents

I. Research Objectives

As originally proposed, the research objectives for the first year of AFOSR Grant 86-0082 were as follows:

1) Explore Variable Mach Number Effects on Swept Interactions

It was proposed to perform a parametric series of experiments using the swept compression corner and semicone shock generator geometries over the range $2.0 \leq M_\infty \leq 4.0$. These experiments will comprise "footprint" measurements via surface streak patterns and pressure distributions as well as flowfield visualizations via conical shadowgraphy and the localized vapor-screen technique. The defining angles of the swept corner generators will span the ranges $0 \leq \lambda \leq 70$ degrees and $10 \leq \alpha \leq 70$ degrees. Specific (α,λ) combinations will be chosen during the course of the experiments in order to locate the flow regime boundaries and focus on the critical phenomena revealed by the Mach number variation. The defining angles of the semicone generators will span the range $15 \leq \alpha \leq 40$ degrees, and will be chosen so as to produce weak, intermediate, and strong interactions at each value of M_∞. The Mach number itself will be given specific values of 2.0, 2.5, 3.0, 3.5, and 4.0 unless the progress of the experiments dictates that other values would be more useful to the goals of the study.

These experiments will be designed to answer the important questions concerning variable Mach number effects on swept interactions. In particular, the relative importance of M_∞ vs. M_N in establishing interaction similarity will be examined and assessed. As discussed earlier, there is strong evidence that M_N is a primary similarity parameter for swept interaction strength with fixed M_∞ and variable shock generator geometry. There is also very limited evidence that M_N alone may be sufficient to achieve this similarity despite variations in M_∞. The author has extracted the few available indications of variable Mach number effects in fin-generated interactions in the literature. Though these data are coarse, they seem to obey a similarity rule which connects the interaction response, $\beta_{sepn} - \beta_0$, to M_N according to:

$$\tan(\beta_{sepn} - \beta_0) \simeq (M_N^2 - \text{const})^{0.5}$$

At least, this similarity appears to hold for higher Mach numbers in the range $3.75 \leq M_\infty \leq 5.9$. However, for $M_\infty = 2.95$, where the most detailed data are available from the Princeton experiments, this apparent similarity seems to break down. Little more can be said about this until more detailed data are available, except to add that Inger's triple-deck analysis indicates both M_N and M_∞ must be taken into account in any such similarity scheme. Inger explains this claim by noting that substantial changes occur in the incoming boundary layer profile with variable M_∞ which cannot simply be accounted for by M_N alone. The experiments proposed here will be aimed, in part, at resolving this question for Mach numbers up to 4.

These experiments will also address the question of the M_∞ effect on the Reynolds number exponent "a" in the similarity law derived in earlier work. As it stands, we know that this exponent takes on a value of -1/3 for $M_\infty = 3$, but there are no data available for other Mach numbers. The nature of the flow mechanism responsible for "a" thus cannot be explored until more experiments are

done. These experiments will require that both the wind tunnel wall boundary layer ($\delta \simeq 18$ mm) and a boundary layer developed on a flat plate ($\delta \simeq 5$ mm) be used in order to cover a Reynolds number range at each Mach number considered.

Finally, the proposed experiments will locate the cylindrical/conical flow regime boundary for swept corner interactions at Mach 4. This knowledge, coupled with that already available at Mach 3, should allow us to find the behavior of the effective detachment Mach number, M_{slip}. If successful, this strategy will finish the currently incomplete explanation of this flow regime boundary. The author hopes to work closely on this issue with Prof. Inger, who will be considering the same problem from an analytical standpoint with AFOSR support. Note that a number of swept corner (α,λ) combinations must be tested to locate the cylindrical/conical boundary at each Mach number value one chooses. We will therefore not attempt to do so at all five M_∞ values unless this proves necessary to satisfy the research goals. (Some limited boundary data are already available at Mach 2 from the Princeton tests.)

This plan for variable Mach number swept interaction research involves an extensive experimental test matrix. This is the major task proposed for the first year of AFOSR-supported research. This work will be integrated closely with a smaller study of Mach number effects on fin-generated interactions which is currently in progress with support from NASA-Ames.

2) Explore Possible Facility Effects

This important issue requires only a relatively small number of experiments. It is proposed to repeat a few selected points from the extensive Mach 3 database developed at Princeton. These check points should include, for example, heavily-studied interactions like the sharp fin at α = 10 degrees and the α = 24, λ = 40 degree swept corner. Interaction footprint pressures and streak patterns should be adequate for this purpose. A critical comparison will then be made between these results and those obtained at Princeton. While significant differences are not expected, any global disagreement of these similar experiments in different facilities would signal a potentially serious problem. If this should occur, the next step would then be planned in consultation with AFOSR. Prof. Bogdonoff of Princeton has encouraged this effort and has agreed to cooperate with us in carrying it out.

Though not proceeding exactly as originally proposed and discussed above, the research effort has been successful in both of the stated objectives. Our progress and results for the first year of the subject Grant are described in the following section. Further, a publication covering these results is included in the Appendix.

II. Status of the Research - Accomplishments and Progress

1) Variations from Original Research Plan

a) Test Rig Fabrication

As planned, the research effort involved a parametric study of a wide variety of different (α,λ) combinations of swept compression corners. Similar work done earlier at Princeton under AFOSR support required the fabrication of over 50 individual swept corner models. The compound angles of these models make them individually expensive to machine. Further, dismounting and remounting such individual models was very time-consuming in the Princeton experiments. Therefore, we decided to attempt to improve upon this procedure by designing and fabricating a variable-sweep mechanism which would allow a model of given α to be preset at any desired sweep angle in the wind tunnel test section. By this means the number of required test models could be reduced from more than 50 to about 4.

The design of this variable-sweep mechanism proved to be nontrivial. In order to maintain the swept corner apex at a fixed position, a quadrant-type drive arm was designed to protrude from the test section sidewall. This called for the fabrication of a new sidewall as well. Further, loads on the model during tunnel startup and shutdown required a proper stress analysis of the variable-sweep mount in order to avoid a possible failure. In all, several months passed before a satisfactory design was reached. Drawings of this mechanism were provided to the AFOSR Program Manager in a previous, informal report.

Upon completion of the design stage, the variable-sweep drive was put out for machine shop bids and was awarded to a local non-University shop. An extended period was required for fabrication, including two mid-stream design changes necessitated by machining difficulties. The completed mechanism was finally received near the end of 1986, rather late in the Grant period. Photographs of its installation in the Penn State supersonic wind tunnel are shown in Figs. 1 and 2.

In summary, the choice of a variable-sweep drive over an array of fixed models probably did not result in a lower overall cost. However, the improvement in ease of testing a variety of (α,λ) combinations is dramatic. On this basis the decision appears to have been a sound one.

b) Experiments on Mach Number Effect

The effect of the delays discussed above was that the ambitious swept corner test program originally proposed could not be completed during the first year of the Grant. A more limited test series has been conducted, with results described in a later section. Meanwhile, while awaiting hardware fabrication, we proceeded to pursue the proposed Mach number effect study in spirit by considering fin-generated interactions rather than those generated by swept

corners. The apparatus with which to conduct variable-M_∞ fin interaction experiments was available, having been constructed previously under other support. An extensive test matrix was carried out using sharp, unswept fins at angles of attack between 0 and 20 degrees at Mach numbers of 2.5, 3.0, 3.5, and 4.0. (Experiments below Mach 2.5 proved not feasible due to wind tunnel stalling with the flat plate and test model in place.)

This turn of events appears to have been fortuitous. The variable-M_∞ fin experiments have been highly successful and fundamental knowledge of Mach number effects on swept interactions has been gained (to be described below). Since fin interactions involve one less free parameter (λ) than swept corner interactions, it now seems clear that they should be considered first, yielding knowledge of interaction Mach number effects more directly. There certainly remain unanswered questions in the case of the swept corner geometry, however. We are pursuing these questions by way of a limited set of continuing experiments during the second year of the subject Grant.

c) Experiments to Assess Facility Effects

This objective of the proposed work has been carried out essentially as planned. Comparisons have yet to be made between current swept corner results and those of the earlier Princeton work. However, a strong test case is available for fin interactions. The results are discussed below.

2) Research Results

a) Experiments on Mach Number Effect

The sharp fin interaction experiments we have carried out over ranges of both M_∞ and α have been analyzed thoroughly. The results have been reported in detail in a recent AIAA Paper which is included in the Appendix of this Report. This section, then, serves as a summary of the results.

In our research objectives, we raised the question of the relative influence of M_∞ and M_N on swept interaction similarity. The observed result is that *both are important, ie*, fin interactions may not be explained purely on the basis of either parameter. Further, we found that framing the results in terms of M_∞ and M_N is not the most straightforward way to understand them. Instead, we found that the effect of variable Mach number is accounted for most readily by referencing the results to the local undisturbed Mach angle, μ_∞, and the fin angle of attack, α. This simplification results from taking advantage of the symmetry of the space curve which relates shock angle to fin angle and Mach number.

Having accomplished this, we find that the Mach number effect over the range studied is *almost entirely inviscid*. In other words, it is explainable simply in terms of the sweepback which occurs with rising Mach number through the oblique-shock relations. When this is removed, an extremely weak, almost vanishing Mach number effect remains. We thus conclude that the effect of compressibility on the turbulent-flow aspect of swept shock interactions is *vanishingly weak in the supersonic regime*. Within our experimental range, Morkovin's hypothesis is strongly supported. Of course, we recognize that continuing to increase M_∞ into the hypersonic range would bring on a different result.

Further, our results show that the linear growth of interaction size with shock strength, observed by previous investigators, is inaccurate. In fact, the interaction extent appears to grow linearly with fin angle, α, at all Mach numbers tested. Since shock strength (expressed by the shock angle β_0) is clearly not linear with α, it cannot then be that β_0 and the interaction extent are linearly related. In fact, the differences are small over the ranges of parameters covered by previous investigators, which helps explain the misconception previously held by them and by our own research team. However, recognizing the nonlinear relation between shock strength and interaction extent now permits a broader understanding of the phenomenon. *The interaction behavior for very weak and very strong shocks is now much more clearly understood.*

Finally, detailed comparisons have been made with Navier-Stokes solutions carried out by Horstman of NASA-Ames. The salient feature of these comparisons is that *the CFD predictive ability deteriorates as swept interactions grow stronger.* "Stronger," in this context, is a condition which occurs if α is increased at fixed M_∞ and also if M_∞ is increased at fixed α. One may surmise, then, that few cases will be predicted adequately with current Navier-Stokes codes at hypersonic Mach numbers. From the limited CFD results now becoming available for hypersonic interactions, this appears to be the case.

b) Experiments to Assess Facility Effects

According to the stated objective, we have duplicated the test conditions of previous Princeton experiments for sharp fin interactions at Mach 2.95. These experiments were done by Frank K. Lu, a Ph.D. candidate in our group. Coincidentally, Mr. Lu's M.S. degree work at Princeton several years ago included identical measurements in the Princeton 20x20 cm facility. This constitutes a particularly well-controlled test of facility effects, namely: *the same test geometry, M_∞, Re_δ, and investigators, but a different wind tunnel.*

Interaction "footprint" flow visualization data from our current tests and the previous Princeton experiments were directly compared by way of overlays. The two data sets were found to be essentially identical. *We conclude from this that the possibility of facility effects need not be a cause for concern.*

c) Swept Compression Corner Experiments

As mentioned previously, only early results are available from the swept corner test series at this point. Thus we are not yet able to address the substantive questions raised in the research objective discussion of swept corner interactions. However, the experiments are progressing well and high-quality results are being generated. Examples of interaction footprint results at Mach 3.5 and $\alpha_N = 20°$ for a range of sweepback angles, λ, are shown in Figs. 3 through 7.

3) Progress and Plans for Second-Year Effort

a) Optical Study of Interaction Flowfield Structure

The keystone of our second-year research under the subject Grant is the application of the unique abilities of our group in optical flow imaging and diagnostics to understand the *flowfield* structure of swept interactions. We have already made progress in that direction.

From our consideration of previously available data on flowfield structure, one fact seems clear: *The choice of streamwise survey planes has seriously compromised the usefulness of available pressure-probe data.* Early in the study of swept interactions, a streamwise/spanwise coordinate system was chosen largely out of ignorance. Unfortunately, the habit has proved hard to break. Only one set of survey data (R. L. Kimmel, Ph.D. Thesis, Princeton, 1987) is known to exist in a more appropriate coordinate frame. Since the interactions in question are highly swept, a streamwise cut becomes awkward and obfuscating. It has the tendency to stretch the flowfield features longitudinally until they become unrecignizable. Further, none of the investigators who surveyed in streamwise planes went far enough downstream. Since numerous results have shown the quasi-conical symmetry of swept interactions, it now seems clear that *the "natural" coordinate system is an orthogonal one running tangential and normal to the swept shock wave. For maximum clarity, all diagnostics which "cut" through the interaction should do so in the direction normal to the shock.*

Early in the second year of our research effort, we have begun laser light-screen imaging experiments of fin-generated interactions. This is accomplished by expanding a 4-Watt Argon-ion laser beam into a thin sheet using a cylindrical lens. This sheet illuminates a plane normal to the swept shock wave. Moisture is added to the test gas, resulting in condensation which scatters the laser light. This can be observed and recorded as a "cut" through the interaction structure.

Such a result is shown in Fig. 8, the laser light-screen image of the flowfield structure of a Mach 3.5, $\alpha = 18°$ fin interaction. This result is a preliminary one which does not copy well, so white lines have been added to show flow structural boundaries, and the freestream, region A, has been darkened. Region B is the inviscid flow behind the planar fin shock well above the interaction. C denotes the intersection of the light sheet with the fin. Region E is bounded below by the separation vortex D, above by the planar separation shock, and to the right by the rear leg of the bifurcated-shock "λ"-foot. *Region F is an enigma.*

No survey data exist with sufficient resolution to explain region F. The boundary between regions F and B appears as a sharp curved line, but no such feature is resolved in the available survey data. *We hypothesize that this feature is a conical shock wave,* based on its appearance and the properties of regions F and B which it bounds. However, further experiments and analysis are required to properly test this hypothesis.

In any case, the nature of the flowfield in the vicinity of region F is not understood at present. We will attempt to understand it and its relationship with the rest of the flowfield during the current contract year. Our 3D holographic interferometry capability is expected to play a key role in this effort.

Note, in particular, that *computed flow predictions give no help in understanding this flowfield structure.* The grid resolution away from walls in the present-day computations is not nearly fine enough to resolve the discrete flowfield features shown in Fig. 8. The situation is one in which both pointwise measurements and numerical solutions are inadequate to answer the question. *Flow visualization is necessary to do the job.*

b) Laser-Interferometer Skin Friction Measurements

A second objective of our ongoing AFOSR-sponsored research is to obtain high-quality skin friction data in swept interactions. The Laser Interferometer Skin Friction meter (LISF) appears to be the only available instrument which can do this successfully. Only four such instruments are known to exist in the world, and *the Penn State instrument is the only one of these which can function in high-speed flows*. We have spent 3 years under NASA-Lewis support in developing this capability. A recent paper from our group gives the details of what is required for LISF measurements in compressible flows. This paper will be published in an upcoming AGARDograph to appear in late 1987 or early 1988.

At present we are having fabricated the ceiling-mounted optical window necessary to make LISF measurements in swept interactions. (This item was specifically called out in the second-year Grant budget request.) Our goal is to conduct measurements in shock-normal coordinates for the following cases: M_∞ = 3, fin α = 10° and 18°. Another case at a higher Mach number is also planned. Primarily, we hope to gain a better understanding of the flow phenomenology from these data (no such measurements have ever been made). Secondarily, the results should provide an important benchmark for CFD predictions.

III. Publications

Settles, G. S., and Dolling, D. S., "Swept Shock Wave-Boundary Layer Interactions," in "Tactical Missile Aerodynamics," eds. M. J. Hemsch and J. N. Nielsen, Vol. 104 of *AIAA Progress in Astronautics and Aeronautics* Series, September, 1986, pp. 297-379.

Lu, F. K., Settles, G. S., and Horstman, C. C., Mach Number Effects on Conical Surface Features of Swept Shock Boundary-Layer Interactions, *AIAA 19th Fluid & Plasma Dynamics & Lasers Conf.*, Honolulu, June 1987, AIAA Paper 87-1365.

IV. Personnel

Principal Investigator

Prof. Gary S. Settles

Graduate Research Assistants

Joseph Hsu (supported by the subject Grant)

Kwang-Soo Kim (supported by the subject Grant)

Frank K. Lu (supported in part by the subject Grant and in part by NASA-Ames Interchange Agreement NCA2-192)

(Each of these students is a current Ph.D. candidate in the Mechanical Engineering Department.)

V. Interactions

1) Spoken papers presented at meetings, conferences, and seminars

a) Lu, F. K., Settles, G. S., and Horstman, C. C., Mach Number Effects on Conical Surface Features of Swept Shock Boundary-Layer Interactions, *AIAA 19th Fluid & Plasma Dynamics & Lasers Conf.*, Honolulu, June 1987, AIAA Paper 87-1365. (Presented by F. K. Lu)

b) Settles, G. S., "Shock Wave/Boundary Layer Interactions, Flow Visualization, and Instrumentation," Seminar presented at USAF Arnold Engineering Development Center, Tullahoma, TN, March 20, 1987.

c) Settles, G. S., "Application of Schlieren Optics in Fluid Mechanics and Heat Transfer," Seminar presented at Lehigh University, *Seminars in Engineering Science Series*, Feb. 20, 1987.

2) Consultative and Advisory Functions

a) PI attended AIAA/ASME 4th Fluid Dynamics, Plasma Dynamics, and Lasers Conference, Atlanta, GA, May 12-14, 1986. Attended Shock/Boundary Layer Interaction Session, 3rd High Speed Turbulent Boundary Layer Workshop, and held discussion with many attendees involved in similar research (including C. C. Horstman, D. D. Knight, D. S. Dolling, & G. R. Inger).

b) Dr. C. C. Horstman of NASA-Ames Research Center visited our group on May 19, 1986. He delivered a seminar on hypersonic research and detailed discussion of shock/boundary layer interaction problems were held.

c) PI visited Princeton Gas Dynamics Lab on Aug. 4, 1986 and held discussions with Prof. S. M. Bogdonoff and Mr. R. L. Kimmel on shock/boundary layer interaction problems.

d) PI attended the 4th International Symposium on Flow Visualization, Paris, August 26-29, 1986. Many discussions were held with international investigators who are applying advanced optics in high-speed flows. These included discussions with Drs. C. Veret and S. Surget, ONERA; Dr. Nishio of Kobe Univ., Japan; and Prof. W. Merzkirch of Univ. Essen, FRG.

e) Prof. G. R. Inger of Iowa State University visited our group on October 10, 1986. He delivered a seminar on triple-deck research and detailed discussions of shock/boundary layer interaction problems were held.

f) Dr. C. C. Horstman of NASA-Ames Research Center visited our group on October 20-21, 1986. Detailed discussion of shock/boundary layer interaction problems were held, especially including CFD comparisons with our data. All members of our group were involved.

g) Dr. James Daywitt of GE Reentry Systems Div. visited our group on October 28, 1986. He delivered a seminar on hypersonic research and was given a tour of our facilities.

h) Dr. James Reichman of ONR visited our group on November 5, 1986. He was given a tour of our facilities and discussions of high-speed propulsion research were held.

i) Dr. Lyle Long of Lockheed/CA Co. visited our group on November 11, 1986. He delivered a seminar on hypersonic research and was given a tour of our facilities. Discussions of cooperative shock/boundary layer interaction research in Lockheed's hypersonic wind tunnel were held.

j) PI visited Dr. James D. Wilson, Program Manager of the subject Grant, at AFOSR on November 20, 1986. Research progress was reviewed and discussions of a possible second-year effort were held.

k) The Cable News Network carried a 3-minute story on the PSU Supersonic Wind Tunnel Laboratory several times during the week of Dec. 8, 1986. The wind tunnel facility, optical instrumentation, and shock/vortex interaction experiments were featured.

l) PI attended AIAA 25th Aerospace Sciences Meeting, Reno, NV, Jan. 12-15, 1987. Attended sessions on shock/boundary layer interactions and related topics. Held discussions with co-workers in this research area including S. M. Bogdonoff, M. Holden, C. C. Horstman, D. D. Knight, D. S. Dolling, & G. R. Inger).

m) All members of our research group attend a short course given by Prof. John D. Anderson on hypersonics, Jan. 19-20, 1987, at PSU.

n) Dr. Klaus Schadow of the US Naval Weapons Center gave a seminar on ramjet propulsion at PSU on Feb. 11, 1987. He was given a tour of our Laboratory and discussion were held on optical diagnostics and supersonic mixing problems.

o) Dr. David Polling of Boeing Vertol gave a seminar at PSU on Feb. 10, 1987, on the subject of blade/vortex interactions. He was given a tour of our Laboratory and mutual interests in shock/vortex interaction problems were discussed.

p) Prof. R. C. Nelson of Notre Dame Univ. gave a seminar at PSU on Feb. 12, 1987, on the subject of vortex flow visualization. He was given a tour of our Laboratory and mutual interests in flow visualization techniques were discussed.

q) PI visited USAF Arnold Engineering Development Center, Tullahoma, TN, March 20, 1987. Subject: shock wave/boundary layer interactions, flow visualization, facilities, and instrumentation. Contacts: L. Trimmer, J. O'Hare, R. K. Matthews, V. Cline (CALSPAN).

VI. Figures

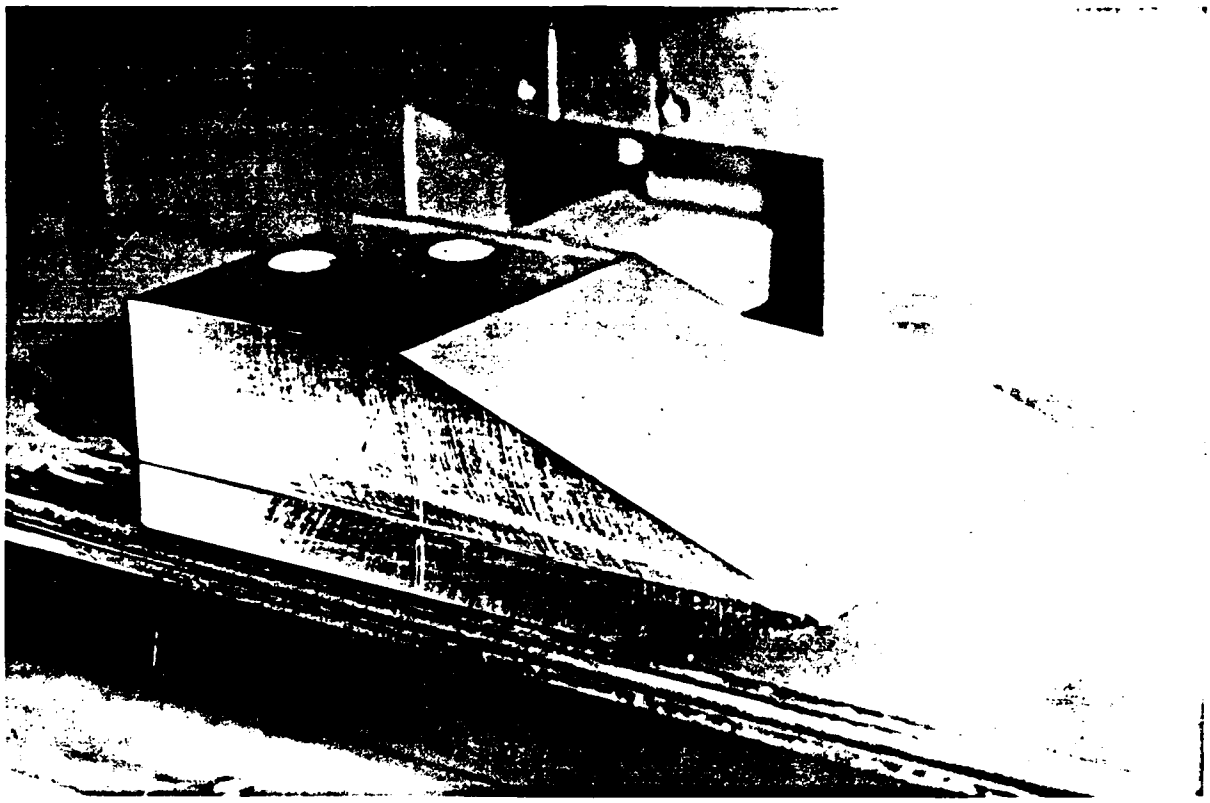

Fig. 1 - Photo of Swept Corner Model on Flat Plate with Variable Sweep Arm Installed.

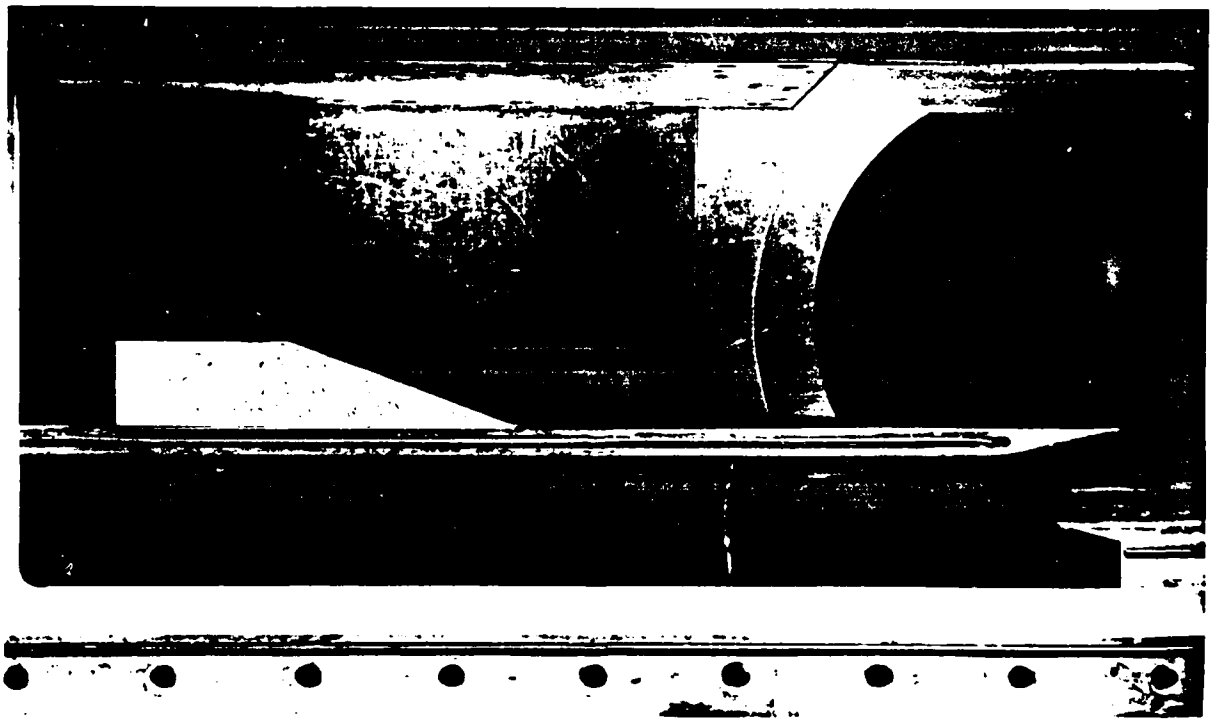

Fig. 2 - Side View of Swept Corner/Flat Plate Installation in PSUSWT.

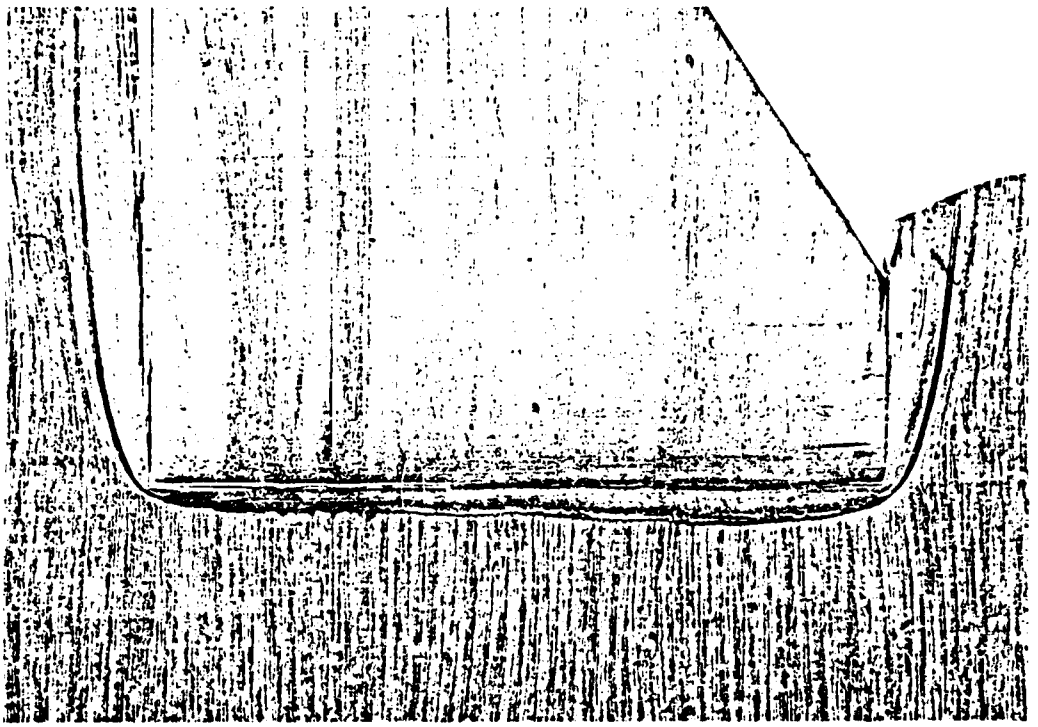

Fig. 3 - Swept Corner Footprint Trace, $M_\infty = 3.5$, $\alpha = 20°$, $\lambda = 0°$

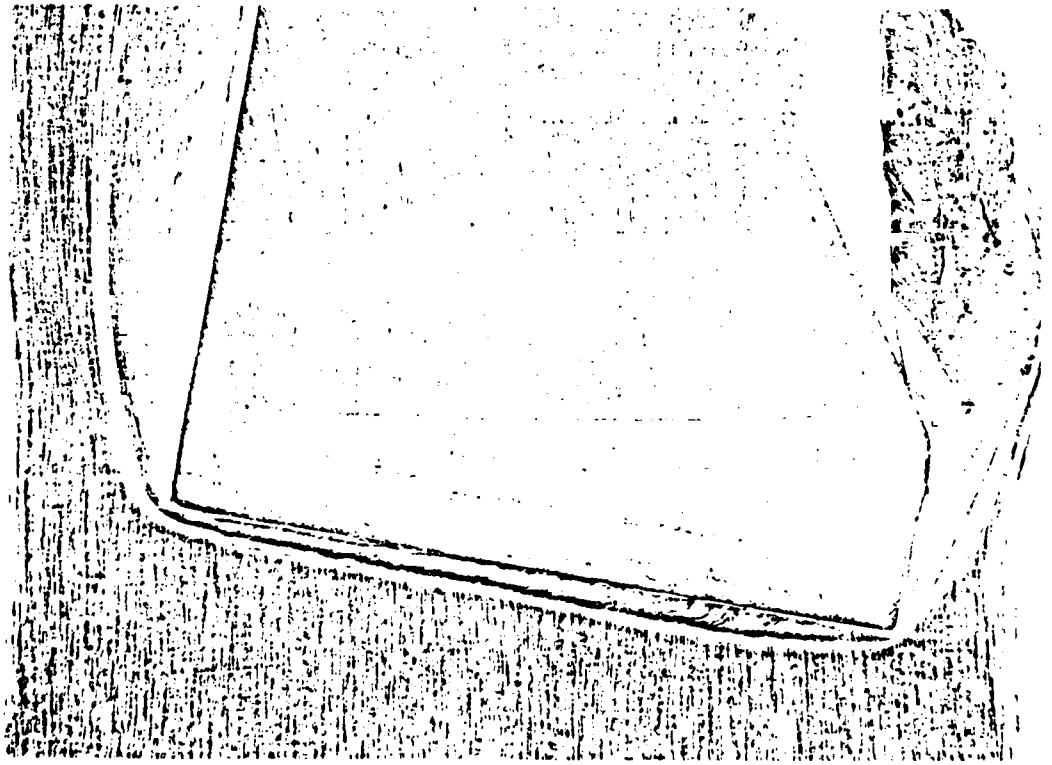

Fig. 4 - Swept Corner Footprint Trace, $M_\infty = 3.5$, $\alpha = 20°$, $\lambda = 10°$

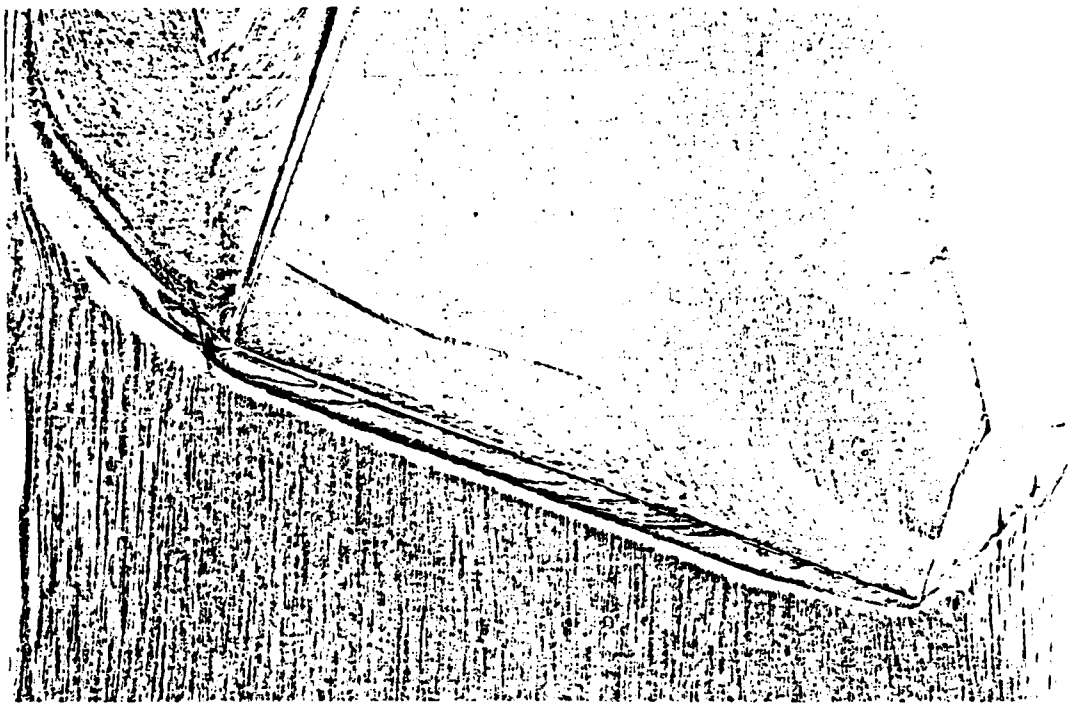

Fig. 5 - Swept Corner Footprint Trace, $M_\infty = 3.5$, $\alpha = 20°$, $\lambda = 20°$

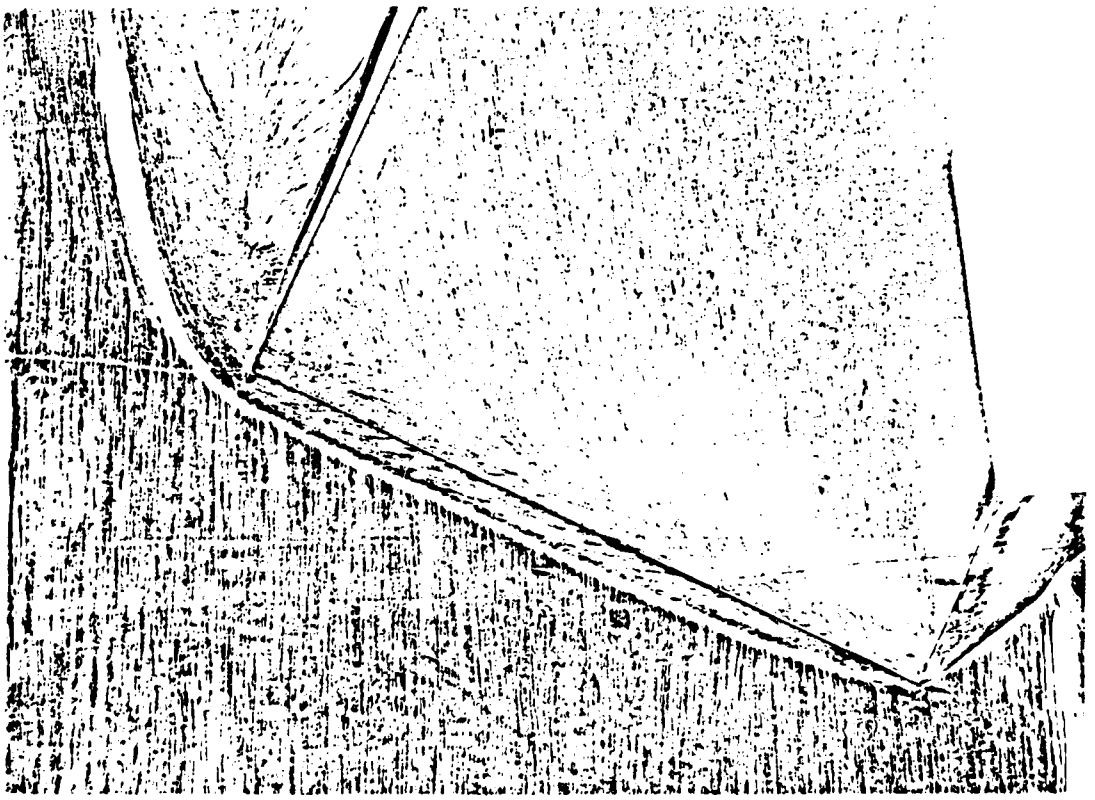

Fig. 6 - Swept Corner Footprint Trace, $M_\infty = 3.5$, $\alpha = 20°$, $\lambda = 25°$

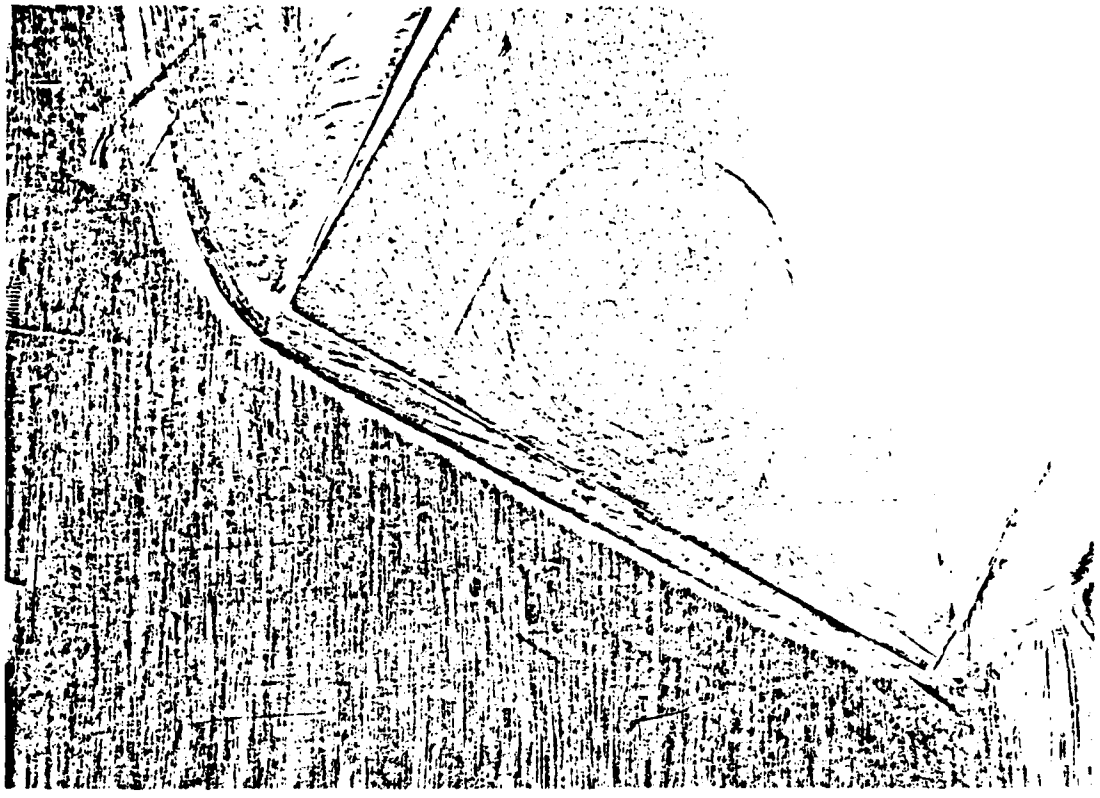

Fig. 7 - Swept Corner Footprint Trace, $M_\infty = 3.5$, $\alpha = 20°$, $\lambda = 30°$

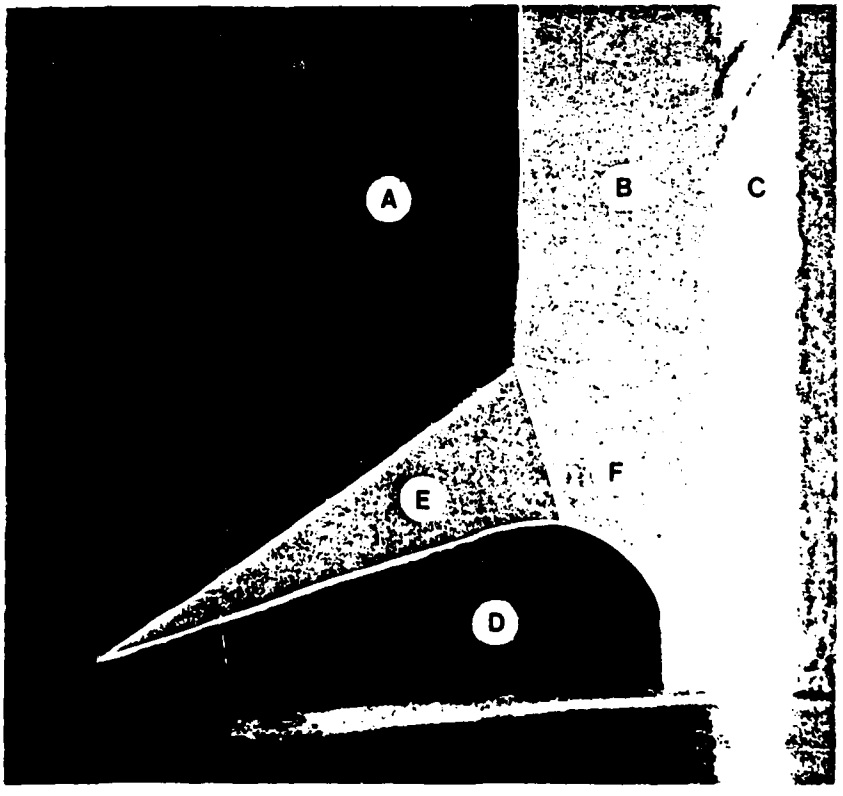

Fig. 8 - Laser Light-Sheet Photo of $M_\infty = 3.5$, $\alpha = 18°$ Fin Interaction.

VII. Appendix

AIAA-87-1365

Mach Number Effects on Conical Surface Features of Swept Shock Boundary-Layer Interactions

F. K. Lu and G. S. Settles,
The Pennsylvania State University,
University Park, PA;
and
C. C. Horstman,
NASA Ames Research Center,
Moffett Field, CA.

AIAA 19th Fluid Dynamics, Plasma Dynamics and Lasers Conference

June 8-10, 1987/Honolulu, Hawaii

AIAA-87-1365

Mach Number Effects on Conical Surface Features of Swept Shock Boundary-Layer Interactions

F. K. Lu* and G. S. Settles,† Pennsylvania State University, University Park, PA, and
C. C. Horstman‡ NASA Ames Research Center, Moffett Field, CA

Abstract

A joint experimental and computational study is made of the shock-wave turbulent boundary-layer interaction generated by sharp fins, with emphasis on Mach number effects. The Mach number range is from 2 to 4 and the unit Reynolds number is from 50 to 80 $\times$ 10^6 per meter. Fin angles are varied from 4° to 22°. Surface-flow patterns are obtained using a color surface-flow visualization technique. The results show that the "upstream-influence response" in the conical, farfield region is a function of the freestream Mach number and the shock strength. A new interpretation of the behavior of the upstream influence with changes of the inviscid shock angle is given. Agreement between the experimental and the computed upstream-influence lines becomes poorer for stronger interactions, with the computations underpredicting the upstream-influence line.

Nomenclature

a, b = constants in power of Re_δ in Reynolds-number scaling law, see Equation (1a)
k_1, k_2 = constants in β_{II} correlation, see Equation (3)
(l_s, l_n) = orthonormal coordinate system based on the inviscid shock-wave trace on the test surface (Figure 2b), mm (in.)
L_n = $(l_n/\delta)\, Re_\delta{}^a$, non-dimensional distance measured normal to the inviscid shock-wave trace on the test surface
L_s = $(l_s/\delta)\, Re_\delta{}^b$, non-dimensional distance measured along the inviscid shock-wave trace on the test surface
M_n = $M_\infty \sin\beta_{\infty}$, Mach number normal to the inviscid shock-wave trace on the test surface
M_∞ = incoming freestream Mach number
M_2 = freestream Mach number downstream of shock
p_{∞} = stagnation pressure of incoming stream, MPa (psia)
p_1 = incoming freestream static pressure, MPa (psia)
p_2 = freestream static pressure downstream of shock, MPa (psia)
p_r = p_2/p_1, inviscid pressure ratio across shock
r = distance measured from the virtual origin (Figure 2b), mm (in.)
Re = unit Reynolds number, m^{-1} (/ft)
Re_δ = Reynolds number based on the local, undisturbed boundary-layer thickness
T_w = wall temperature, K (°R)
T_{∞} = freestream stagnation temperature, K (°R)
α = angle made by fin with respect to the incoming freestream direction, deg.
β = angle made by surface-flow features with respect to the incoming freestream direction, deg.
β_{∞} = angle made by inviscid shock-wave trace on the test surface with respect to the incoming freestream direction, deg.
δ = local, undisturbed boundary-layer thickness, mm (in.)
$\Delta\beta_{II}$ = $(\beta_{II} - \mu_\infty)$, deg.
$\Delta\beta_{\infty}$ = $(\beta_{\infty} - \mu_\infty)$, deg.
κ_1, κ_2 = constants in scaling of $\Delta\beta_{II}$ with $\Delta\beta_{\infty}$, see Equation (12)
λ = fin leading-edge sweepback angle, deg.
μ_∞ = $\arcsin(1/M_\infty)$, Mach angle of the incoming freestream, deg.

* Graduate Research Assistant, Mechanical Engineering Department, Member AIAA.
† Associate Professor, Mechanical Engineering Department, Member AIAA.
‡ Assistant Branch Chief, Experimental Fluid Dynamics Branch, Associate Fellow AIAA.

Subscripts

i	= inception
max	= highest fin angle-of-attack
U	= upstream influence
∞	= incoming freestream conditions

Introduction

Shock-wave boundary-layer interactions have received renewed and urgent interest, due in part to current developments in hypersonic flight vehicles. Although fundamental research on such problems in the past concerned mainly two-dimensional interactions, the last decade or so has seen progress on the problems of three-dimensional interactions. The latest research into these complicated fluid dynamics problems was recently reviewed by Settles and Dolling[1] who broadly divided three-dimensional shock-wave boundary-layer interactions into semi-infinite interactions and non-semi-infinite interactions. Within the class of semi-infinite interactions is a subclass of dimensionless interactions of which a shock generator mounted perpendicularly to a flat surface forms an archetypical family (Figure 1). The geometry depicted in Figure 1 is also commonly called a "fin" with obvious connotations.

Brief Review of Related Studies

For reasons of practical importance, past studies of fin-generated interactions have concentrated on interactions involving turbulent boundary layers. A useful technique in these studies is the use of surface-flow visualization; an example of a surface-flow pattern is shown in Figure 2a while the key features in Figure 2a are identified in Figure 2b. The fin, placed at an angle α to the incoming stream, generates an inviscid shock wave which impinges the test surface at an angle β_∞. The upstream-influence line is the location of the onset of the interaction. The separation line, if it occurs, marks a severe turning of the oil flow resulting in a convergence of the surface streaks. This is believed to indicate that an open boundary-layer separation exists. Associated with the separation line is an attachment line. Within the separated region bounded by the separation and attachment lines is a strong, swept vortical flow. Separation occurs only when the shock provoking the interaction is sufficiently strong. Early studies showed that the incipient separation condition occurs when $M_n \approx 1.2$ or, equivalently, $p_r \approx 1.5$. For the strongest interactions, a secondary separation is also observed although not much is known about this phenomenon.

Settles and Lu[2] found that the surface-flow pattern in fin-generated interactions showed an "inception region" near the fin leading edge and a farfield region further away (Figure 2b). The surface features in the farfield appear to radiate from a "virtual origin," thus displaying conical symmetry. This conical symmetry was also found analytically by Inger[3] and was alluded to by Hayes[4] and Zubin and Ostapenko[5] in their experimental studies. Inger found that, although the boundary-layer growth is not conical, the conical nature of the inviscid freestream nonetheless forces the interaction to tend toward a conical form in the farfield. From the experimental studies, therefore, an appropriate coordinate system to quantify the surface features of such interactions (at least for the region between the upstream-influence line and the inviscid shock-wave trace), is a polar coordinate system, (r, β), centered at the virtual origin as can be seen in Figure 2b.

An excellent approximation to the polar coordinate system described above is an orthonormal coordinate system, (l_s, l_n), which is also shown in Figure 2b. In this coordinate system, l_s is distance measured along the inviscid shock-wave trace on the test surface and l_n is distance measured normal to l_s.

Dolling and Bogdonoff[6] and Settles and Lu[2] found that the upstream-influence line in a Mach 3 fin-generated interaction obeys the following Reynolds-number scaling law:

$$\left[\frac{l_n}{\delta}\, Re_\delta^{\,a}\right]_U \Big/ M_n = f\left(\left[\frac{l_s}{\delta}\, Re_\delta^{\,b}\right]_U\right), \tag{1a}$$

or

$$\frac{[L_n]_U}{M_n} = f\left([L_s]_U\right) \tag{1b}$$

In Equation (1a), the empirically derived constants, a and b, were both found to be equal to 1/3. Equation (1b) was further found to hold for fins with swept leading edges. Subsequently, Settles[7] found that the

nondimensional inception length to conical symmetry for Mach 3 fin-generated interactions, L_{s_i}, is related to β_o by

$$L_{s_i} \approx 1130 \cot \beta_o. \tag{2}$$

Thus, Settles' study identified the dependence of l_{s_i} on both viscous and inviscid parameters.

In the conically symmetric region, there have been attempts to understand the behavior of these surface features.[2,8-10] Basically, these studies found that the salient indicator of interaction "response," the upstream-influence angle, β_{II}, could be expressed as

$$\beta_{II} = k_1 \beta_o - k_2. \tag{3}$$

where $k_1 = 1.74$ and independent of Mach number, whereas k_2 is a decreasing function of Mach number.[10] A more physical correlation, based in part on Equation (1*b*), was given by Settles and Lu[2] for Mach 3 interactions as

$$(\beta_{II} - \beta_o) = \arctan(0.26 \sin \beta_o). \tag{4}$$

The linearity of β_{II} with β_o, expressed by Equations (3) or (4) appears valid for fins with swept as well as unswept leading edges over a limited range of fin angle, α.

The study by Settles and Lu[2] also found that other key surface-feature angles, such as β_{S1}, β_{A1} and β_{S2} (see Figure 2b), increase with shock strength. In addition, just as for β_{II}, these angles obtained with upright fins correlated with those obtained with fins having swept leading edges. Settles and Lu concluded that planar or weakly curved inviscid shocks of the same β_o produce essentially equivalent interactions. This is because the effect of the shock is a local one in the immediate vicinity of the boundary layer. In this local region, the inviscid shocks have large radii of curvature regardless of fin leading-edge sweepback.

Other than experimental studies, numerical predictions of the interaction using approximations to the Navier-Stokes equations were recently performed by several investigators including Horstman.[11] Horstman's results revealed that a flat vortex exists when the boundary layer is separated, a fact that had already been observed experimentally.[2,8] The computed skin-friction lines and surface pressure distributions show that the farfield surface features are conically symmetric. However, these computed features are more highly swept than the corresponding experimental features at the same shock strength. *Agreement with experiments* becomes poorer as the shock strength increases. Agreement with experiments using a thin boundary layer (3 mm) is also poorer than agreement with experiments using a thick boundary layer (13 mm). At present, the reasons for the lack of agreement are unknown. Two possible reasons are an insufficient mesh resolution and an inappropriate turbulence model.

Present Study

As noted above, fin-generated interactions have been relatively well studied at Mach 3. However, no comprehensive study has been done through a wide Mach number range. The effect of Mach number on the interaction is therefore largely unknown and is a question that needs to be answered. Previous studies, ranging from Mach 2 through 11 (such as References 4 and 12 through 14), are generally inadequate for this purpose from our present standpoint. The reason for this is that insufficiently detailed measurements were reported. This is especially so of the upstream influence even though its determination is important in both practical and theoretical terms.

In addition, most fin interaction studies were done at one or two Mach numbers only and were thus unable to reveal Mach number trends. Some studies were also contaminated by wind-tunnel sidewall interference or were carried out within the inception zone. Data from such experiments obviously cannot be correlated using the otherwise powerful concept of conical symmetry.

A broad, new experimental program was therefore devised to explore fin-generated interactions through a Mach number range of 2.5 to 4. Concurrently, computations were performed to judge the ability of the state-of-the-art computational techniques and the latest computers to simulate such flows. The computations were then compared with the experiments. This dual study was designed to address the following important issues:

a. the dependence of the interaction length scales, for example, l_{s_i}, on M_∞ and shock strength;

b. the behavior of the conical region with Mach number change,

c. the effect of Mach number on surface pressure distributions;

d. the changes of the flowfield with Mach number;

e. the possibility of facility effects (since the bulk of existing Mach 3 experimental data was generated in a single facility); and

f. the ability of computational models to predict the interaction.

This paper reports the first phase of this research program which is an analysis of the farfield upstream-influence line revealed by surface-flow visualization.

Experimental Methods

Wind Tunnel and Test Models

The experimental study was done in the Pennsylvania State University Supersonic Wind Tunnel (SWT). This wind tunnel is a blowdown type with a nominal Mach number range from 1.5 through 4. The variable Mach number capability is achieved by way of an asymmetric sliding-block nozzle. The SWT has a test section 150 mm (6 in.) wide, 165 mm (6.5 in.) high and 610 mm (24 in.) long. (Further description of the wind tunnel and the experiments can be found in Lu.[15])

For the present tests, a flat plate, 500 mm (19.5 in.) long, spanning the tunnel, was mounted in the test section to provide the interaction test surface. A fin model with a 10° sharp leading edge was placed with its tip 216 mm (8.5 in.) from the plate leading edge and 26.2 mm (1.03 in.) from the tunnel sidewall. The fin was 100 mm (4 in.) high, 127 mm (5 in.) long and 6.35 mm (0.25 in.) thick. The fin height of about 30δ was therefore sufficient to ensure that the interaction was a semi-infinite one.[1,16] The length of the fin was chosen to provide the maximum interaction extent while allowing sufficiently large angles-of-attack to be obtained without stalling the wind tunnel.

The fin was held tightly onto the flat plate by a fin-injection mechanism mounted on the tunnel sidewall. A rubber seal at the bottom of the fin ensured that no leakage under the fin occurred during the tests. The fin-injection mechanism pneumatically injected the fin to a preset angle-of-attack, α, once test conditions were established. This was necessary only for tests with α larger than approximately 14°. At lower angles, α was fixed before the run. In the experiments, α ranged from 4° to 22°, the largest value being limited by tunnel stall. The fin angle was determined to 0.1° accuracy using a machinist's protractor.

Test Conditions

The Mach numbers of the experiments were 2.47, 2.95, 3.44 and 3.95. The incoming freestream conditions at these Mach numbers are summarized in Table 1. Since the wind tunnel is a blowdown type, the stagnation temperature decreased somewhat during a run. Typically, for a run of about twenty seconds, the stagnation temperature, T_{o_1}, dropped from 300 K (540°R) to 290 K (520°R). The nominal freestream unit Reynolds number, Re, was held relatively constant throughout the Mach number range at 50 to 80 $\times 10^6$ m^{-1} (15 to 24 $\times 10^6$/ft). In order to achieve this, the tunnel stagnation pressure, p_{o_1}, had to be increased with Mach number as can be seen from Table 1.

Figure 3 is an example of an undisturbed centerline boundary-layer velocity profile in law-of-the-wall coordinates. The figure also shows the Sun-Childs[17] wallwake curvefit to the data. Detailed surveys along the flat-plate centerline and 38 mm (1.5 in.) to each side showed that the boundary layers were two-dimensional. The boundary layers were turbulent and in equilibrium at the test region and were at approximately adiabatic conditions.

Experimental Techniques

Temperature data from thermocouples and pressure data from pressure transducers were digitized and stored in a microcomputer. The computer was used to display tunnel conditions during a test as well as to analyze data. Further data analysis was performed on a mainframe computer.

The surface-flow features were visualized using a kerosene-lampblack technique.[18] In addition, an improvement over this well-tried technique used powdered colored chalk as the pigment material in a kerosene carrier. The colors helped to distinguish some of the important features of the surface flow, particularly the separation line. Spatial data obtained from full-size undistorted images of the surface pattern (preserved

on matte acetate tape) were accurate to 0.5 mm (0.02 in.); these data were also digitized and stored in a microcomputer for analysis. Angular data were accurate to $\pm 0.5°$ for stronger interactions, but accuracy can be as poor as $\pm 3°$ for weak interactions due to difficulty in discerning weak surface-flow features.

Computations

The computations, using the MacCormack explicit, second-order, predictor-corrector, finite-volume method, solve the Reynolds-averaged Navier-Stokes equations with a two-equation k-ϵ turbulence model.[11] Computations were made at Mach 2 and 4 for interactions generated by $\alpha = 5°$, $14°$ and $20°$ fins. Further, for the first time, computations of a swept leading-edge fin-generated interaction were made. Two cases at Mach 3 were considered, namely, interactions generated by an $\alpha = 15°$, $\lambda = 20°$ fin and an $\alpha = 15°$, $\lambda = 40°$ fin.

The Upstream Influence

Discussion of Experimental Results

As a first step in the data analysis, the raw β_{II} data are plotted in Figure 4 against β_{∞}. The line $\beta_{II} = \beta_{\infty}$ in this figure amounts to a lower bound for vanishingly weak interactions. At the other extreme, the largest value of β_{II} for a given M_{∞}, by extrapolation of data, is presumed to correspond to the largest α before inviscid shock detachment, α_{max}. For $M_{\infty} > 2$, β_{∞} is almost constant ($\approx 65°$ to $68°$) for fins at an angle of α_{max}. Therefore, the range of β_{∞} widens as M_{∞} goes up because of a decrease of μ_{∞} rather than an increase of the maximum shock angle. The result is that β_{II}, too, would have a wider range of values.

Figure 4 also shows that, at a given β_{∞}, β_{II} increases with M_{∞}. To obtain the same β_{∞} requires that α increases with M_{∞}. This, therefore, implies that β_{II} in fact increases with the strength of the interaction, regardless of M_{∞}. Conversely, for a given α, β_{II} decreases with increasing M_{∞}. In other words, as M_{∞} increases for a given α, the interaction extent (in angular terms) decreases. Further, since the inviscid shock pressure ratio increases with M_{∞} for a constant α, there will be larger interaction pressure gradients as M_{∞} increases because the pressure rise has to occur over a smaller angular extent. Thus, boundary-layer separation would occur at lower α as M_{∞} increases, a fact which is well documented.[12,14,19]

Dimensional Analysis

In trying to determine Mach-number scaling laws for β_{II}, it is appropriate to begin with dimensional analysis. The functional dependence of β_{II} on the controlling parameters can be written as

$$\beta_{II} = f_{II}\,(l_s,\ \delta,\ Re_{\delta},\ M_{\infty},\ \beta_{\infty})\,, \tag{5}$$

for given T_w/T_{∞} conditions. Note that the fin geometry, given by α, is implicit in β_{∞} since the inviscid shock-wave trace depends on the fin geometry as well as on M_{∞}. Equation (5) can be conveniently rewritten as

$$\beta_{II}(L_s) = f_{II}(Re_{\delta},\ M_{\infty},\ \beta_{\infty}). \tag{6}$$

Since the present study examines Mach number effects, Re_{δ} is held approximately constant so that its effect can be neglected. Further, in the conical farfield region where $L_s > L_{s_{\infty}}$, the explicit geometrical dependence can also be dropped since the effect of fin geometry is felt directly only in the inception zone. Equation (6) is therefore simplified to

$$\beta_{II}(L_s > L_{s_{\infty}}) = f_{II}(M_{\infty},\ \beta_{\infty}). \tag{7}$$

For convenience, the argument of β_{II} is omitted in the subsequent discussion.

For extremely weak interactions, when $\beta_{\infty} \rightarrow \mu_{\infty}$, it is postulated that $\beta_{II} \rightarrow \mu_{\infty}$ is a limiting condition on Equation (7). (Experiments under such circumstances are scarce and difficult to perform and the results have large scatter.) Equation (7) is thus rewritten to properly reference both β_{∞} and β_{II} to their limiting values:

$$(\beta_{II} - \mu_{\infty}) = f_{II}\left(M_{\infty},\ (\beta_{\infty} - \mu_{\infty})\right),$$

or, simplifying the notation,

$$\Delta\beta_{II} = f_{II}\,(M_\infty,\ \Delta\beta_{n}) \tag{8}$$

where $\Delta\beta_{II}$ is a "reduced upstream-influence response" function while $\Delta\beta_{n}$ is a reduced shock-strength function.

Physical Interpretation of Upstream-Influence Scaling

To understand the physics behind the functional relationship given by Equation (8), it is necessary to examine the relationship between β_{n}, α and M_∞, which is a rather complicated one in general:

$$\cot\alpha = \tan\beta_{n}\left[\frac{(\gamma+1)M_\infty^2}{2\left(M_\infty^2\sin^2\beta_{n}-1\right)} - 1\right]. \tag{9}$$

Note that the $\beta_{n} = \beta_{n}(\alpha,\ M_\infty)$ relationship defines a surface in 3-space and that the appropriate segment of this surface for the limited range of the present experiments is almost planar. By inspection, the β_{n}-α curves in this region are approximately parallel to each other and are offset from the α-M_∞ plane by the Mach angle, μ_∞. Thus, subtracting μ_∞ from β_{n} in effect "rotates" the β_{n} surface so that the local region of interest is parallel to the direction of view. This is shown in Figure 5. A second-order least-squares regression of Equation (9) for $2.5 < M_\infty < 4$ and $\alpha < 22°$ yields

$$\Delta\beta_{n} = 0.7\alpha + 0.011\alpha^2. \tag{10}$$

Equation (10) conveniently expresses the fact that β_{n}, referenced to μ_∞, grows nonlinearly with α in the region of present interest.

The upstream-influence angle response function, $\Delta\beta_{II}$, as a function of α is shown in Figure 6. According to the present experiments, it can be observed that $\Delta\beta_{II}$ grows *linearly* with α. Except for a small M_∞-effect, the data approximately follow

$$\Delta\beta_{II} = 1.57\alpha. \tag{11}$$

The physical reason for this linear behavior of $\Delta\beta_{II}$ with α, as compared to the nonlinear behavior of $\Delta\beta_{n}$ with α, is not entirely clear at present. It can be noted, however, that even for separated interactions, the upstream-influence line marks the upstream extent of a compression-wave system in the interaction which coalesces into the forward leg of the familiar "lambda-foot" shock structure. This compression is always expected to be weak compared to the inviscid shock because the flow deflection away from the test surface for separated interactions is limited to 8 to 12°. This weak compression at the upstream limit of the interaction may be responsible for the observed linearity of $\Delta\beta_{II}$ with α.

The linear growth of $\Delta\beta_{II}$ with α and the nonlinear growth of $\Delta\beta_{n}$ with α dictates that $\Delta\beta_{II}$ and $\Delta\beta_{n}$ cannot be linearly related. This is illustrated in a plot of $\Delta\beta_{II}$ versus $\Delta\beta_{n}$ in Figure 7. This figure shows that $\Delta\beta_{II}$ depends primarily on $\Delta\beta_{n}$ with a very weak secondary M_∞ dependence, confirming the results of the dimensional analysis obtained earlier. Thus, to a good approximation, Equation (8) can be simplified to

$$\Delta\beta_{II} = f_{II}\,(\Delta\beta_{n}). \tag{8'}$$

Figure 7 also shows that for weak interactions, $\Delta\beta_{II}$ is more than twice as large as $\Delta\beta_{n}$. But the growth rate of $\Delta\beta_{II}$ decreases with increasing $\Delta\beta_{n}$.

Data scatter in earlier experiments at a single Mach number did not clearly reveal the behavior shown in Figure 7. Many investigators, including the present authors,[2,8-10] modeled the upstream influence behavior linearly by Equation (3). The intercept k_2 was rationalized through arguments claiming rapid interaction growth for very weak shocks. The present results show that the assumption of a linear β_{II} growth with β_{n} is nonphysical. Such an assumption is only approximately valid for a limited range of β_{n}, as can be seen from Figure 7, failing at both the weak and strong limits of shock strength. Instead, from a second-order curvefit to the data, it is proposed that

$$\Delta\beta_{II} = \kappa_1\,\Delta\beta_{n} - \kappa_2\,\Delta\beta_{n}^2, \tag{12}$$

where $\kappa_1 \approx 2.2$ and $\kappa_2 \approx 0.027$. This equation demonstrates the nonlinear growth of β_{II} with β_{n} and accounts for variable Mach number (to first order) by referring both β_{II} and β_{n} to μ_∞. (Note that no

particular physical significance is given to the polynomial form of Equation (12) and that a trigonometric or other dependence would serve as well.)

Equation (12) cannot be extrapolated beyond the present experimental range since doing this would eventually result in β_{II} being less than $\beta_{,,}$, a physically impossible situation. It is, however, hypothesized that in the extreme case of very strong interactions, β_{II} will approach $\beta_{,,}$. This limit is also shown in Figure 7.

Comparison with Computations

As for the present computational solutions, for $2 < M_\infty < 4$, Figure 8 shows that, although the computed $\Delta\beta_{II}$ correlates with $\Delta\beta_{,,}$, the computed results fall below the experimental data. This implies that the computations underpredict the farfield interaction extent. Figure 8 shows that the computed results for interactions generated by $\alpha = 5°$ fins are within the data scatter. But for large α, in which the separated region is large, the computations appear less successful in determining the interaction extent. This can also be seen in a comparison between the experimental surface-flow visualization results (Figure 9a) and the computed surface-friction lines (Figure 9b). It is obvious from these figures that the computed value of β_{II} is smaller than the measured value.

Other Correlating Parameters

There is evidence prior to this study that the upstream-influence location is a strong function of shock strength,[1] although this evidence is based on studies at one or two Mach numbers. The present study shows that to account for the Mach number, the appropriate shock strength parameter must be one which is directly dependent on α and μ_∞ with an otherwise negligible M_∞ dependence. Now, the question is posed as to whether there may be other shock strength parameters that would also be suitable, for example, $C_{p_r} \equiv 2\left(p_r - 1\right)/\gamma M_\infty^2$. However, C_{p_r} shows a Mach number dependence, that is, $C_{p_r} = f\left(\alpha, M_\infty\right)$ so that it is not a suitable parameter. Other parameters which show the desired behavior with respect to α and M_∞ are, for example, $(M_n - 1)/M_\infty$, $\left(p_r - 1\right)/M_\infty$ and $\Lambda \equiv (M_\infty/M_2 - 1)$, a parameter used successfully in two-dimensional impinging shock interactions.[20] The reason why these parameters can be used is, once again, that they are also weak functions of M_∞ for the Mach number range of the present study.

Final Remarks

The present study shows that the Mach number effect on β_{II} is simply accounted for by referencing β_{II} and $\beta_{,,}$ to the Mach angle. Physically, this result stems from the nature of the $\beta_{,,}\left(\alpha, M_\infty\right)$ relationship, wherein the only effect of M_∞ enters through μ_∞ for the present range of variables. The residual M_∞ trend of the data in Figure 7 is extremely weak, such that it is within the overall data scatter. It may be concluded that the upstream-influence response to compressibility effects on the turbulent boundary layer, for $2.5 \leq M_\infty \leq 4$ and adiabatic wall conditions, is of second-order importance and thus may be neglected.

An examination of Figure 7 reveals that a linearized theoretical approach to the upstream-influence problem might be feasible for weak interactions. However, significant deviation from the initial linear growth occurs for $\alpha > 5°$. At the other extreme, for very strong shocks, β_{II} is expected to approach $\beta_{,,}$. The present study, therefore, also answers some of the questions raised by Wang and Bogdonoff,[21] Bogdonoff and Wang[22] and Stalker[23] on whether these interactions are fundamentally conical or cylindrical. The answer is that over a wide range of $\Delta\beta_{,,}$, the interactions are conical. For small values of $\Delta\beta_{,,}$, which result in small values of $\Delta\beta_{II}$, data scatter may give the impression of cylindrical symmetry. Based on the trend of the data, for large values of $\Delta\beta_{,,}$ it is expected that the interaction would approach cylindrical symmetry. Unfortunately, experimental limitations prevent the present investigation and all known prior studies from observing this limit.

Conclusions

The present study shows that the Mach number effect on the farfield upstream-influence line of fin-generated interactions can be simply accounted for by referencing β_{II} and $\beta_{,,}$ to μ_∞. It shows that a suitable shock strength parameter for scaling $\Delta\beta_{II}$ is one which is a function of α and not explicitly of M_∞. The experimental results show that compressibility effects on the turbulent boundary layer are of secondary importance. Computations in the present Mach number range show farfield conical symmetry of

surface features as do the experiments. However, the computations underpredict the angular extent of these features at higher Mach numbers and shock strengths.

Acknowledgments

The experimental work was funded by Grant NCA2-1R589-502 from NASA Ames Research Center, monitored by Dr. C. C. Horstman, and by Grant AFOSR86-0082 from the U. S. Air Force Office of Scientific Research, monitored by Dr. J. D. Wilson. The first author would also like to acknowledge the assistance of Mr. P. J. Barnhart in carrying out some of the experiments. Finally, the authors thank 3M Corporation and Avery Corporation for supplying matte acetate tape in non-standard widths for the surface-flow visualization experiments.

References

1. Settles, G. S. and Dolling, D. S., "Swept Shock Wave/Boundary-Layer Interactions," in *AIAA Progress in Astronautics and Aeronautics: Tactical Missile Aerodynamics*, edited by M. Hemsch and J. Nielsen, Vol. 104, AIAA, New York, 1986, pp. 297-379.

2. Settles, G. S. and Lu, F. K., "Conical Similarity of Shock/Boundary Layer Interactions Generated by Swept and Unswept Fins," *AIAA Journal*, Vol. 23, July 1985, pp. 1021-1027.

3. Inger, G. R., "Spanwise Propagation of Upstream Influence in Conical Swept Shock/Boundary-Layer Interactions," *AIAA Journal*, Vol. 25, February 1987, pp. 287-293.

4. Hayes, J. R., "Prediction Techniques for the Characteristics of Fin-Generated Three Dimensional Shock Wave Turbulent Boundary Layer Interactions," USAF AFFDL-TR-77-10, May 1977.

5. Zubin, M. A. and Ostapenko, N. A., "Structure of Flow in the Separation Region Resulting from Interaction of a Normal Shock Wave with a Boundary Layer in a Corner," *Izvestiya Akademii Nauk SSSR, Mekhanika Zhidkosti i Gaza*, Vol. 14, May-June 1979, pp. 51-58, (Engl. trans).

6. Dolling, D. S. and Bogdonoff, S. M., "Upstream Influence in Sharp Fin-Induced Shock Wave/Turbulent Boundary-Layer Interaction," *AIAA Journal*, Vol. 21, January 1983, pp. 143-145.

7. Settles, G. S., "On the Inception Lengths of Swept Shock-Wave/Turbulent Boundary-Layer Interactions," *Proceedings of the IUTAM Symposium on Turbulent Shear-Layer/Shock-Wave Interactions*, edited by J. Délery, Palaiseau, France, September 1985, Springer-Verlag, Berlin, 1986, pp. 203-213.

8. Settles, G. S. and Kimmel, R. L., "Similarity of Quasiconical Shock Wave/Turbulent Boundary-Layer Interactions," *AIAA Journal*, Vol. 24, January 1986, pp. 47-53.

9. Goodwin, S. P., "An Exploratory Investigation of Sharp Fin-Induced Shock Wave-Turbulent Boundary-Layer Interactions at High Shock Strengths," MSE Thesis, Mechanical and Aerospace Engineering Department Report No. 1687-T, Princeton University, NJ., November 1984.

10. Dolling, D. S., "Upstream Influence in Conically Symmetric Flow," *AIAA Journal*, Vol. 23, June 1985, pp. 967-969.

11. Horstman, C. C., "Computation of Sharp-Fin-Induced Shock Wave/Turbulent Boundary-Layer Interactions," *AIAA Journal*, Vol. 24, September 1986, pp. 1433-1440.

12. Zheltovodov, A. A., "Properties of Two- and Three-Dimensional Separation Flows at Supersonic Velocities," *Izvestiya Akademii Nauk SSSR, Mekhanika Zhidkosti i Gaza*, Vol. 14, May-June 1979, pp 42-50 (Engl. trans).

13. Zheltovodov, A. A., Pavlov, A. A., Shilein, E. H. and Yakovlev, V. N., "Interconnectionship Between the Flow Separation and the Direct and Inverse Transition at Supersonic Speed Conditions," *Proceedings of the IUTAM Symposium on Laminar-Turbulent Transition*, edited by V. V. Kozlov, Novosibirsk, USSR, 1984, Springer-Verlag, Berlin, 1985, pp. 503-508.

14. Zheltovodov, A. A., "Regimes and Properties of Three-Dimensional Separation Flows Initiated by Skewed Compression Shocks," *Zhurnal Prikladnoi Mekhaniki i Tekhnicheskoi Fiziki*, No. 3, May-June 1982, pp. 116-123 (Engl. trans).

15. Lu, F. K., "Mach Number Effects on Fin-Generated Shock-Wave Boundary-Layer Interactions," Ph.D. Thesis, The Pennsylvania State University, to be published.

16. McClure, W. B., "An Experimental Study into the Scaling of the Interaction of an Unswept Sharp Fin-Generated Shock/Turbulent Boundary Layer Interaction," M.S.E. Thesis, Princeton University, January 1983.

17. Sun, C. C. and Childs, M. E., "A Modified Wall-Wake Velocity Profile for Turbulent Compressible Boundary Layers," *AIAA Journal of Aircraft*, Vol. 10, June 1973, pp. 318-383.

18. Settles, G. S. and Teng H.-Y., "Flow Visualization Methods for Separated Three-Dimensional Shock Wave/Turbulent Boundary Layer Interactions," *AIAA Journal*, Vol. 21, March 1983, pp. 390-397.

19. Korkegi, R. H., "A Simple Correlation for Incipient Turbulent Boundary-Layer Separation due to a Skewed Shock Wave," *AIAA Journal*, Vol. 11, November 1973, pp. 1578-1579.

20. Green, J. E., "Interactions Between Shock Waves and Turbulent Boundary Layers," *Progress in Aerospace Sciences*, Vol. 11, edited by D. Küchemann, Pergamon Press, Oxford, U. K., 1970, pp. 235-340.

21. Wang, S.-Y. and Bogdonoff, S. M., "A Re-Examination of the Upstream Influence Scaling and Similarity Laws for 3-D Shock Wave/Turbulent Boundary-Layer Interaction," AIAA Paper 86-0347, January 1986.

22. Bogdonoff, S. M. and Wang, S.-Y., "Comment on 'Conical Similarity of Shock/Boundary Layer Interactions Generated by Swept and Unswept Fins'," *AIAA Journal*, Vol. 24, March 1986, p. 540.

23. Stalker, R. J., "A Characteristics Approach to Swept Shock Wave Boundary Layer Interactions," *AIAA Journal*, Vol. 22, November 1984, pp. 1626-1632.

Table 1 Incoming Freestream Conditions

M_∞	p_o, MPa (psia)	T_o, K (°R)	$Re \times 10^{-6}$, m^{-1} (/ft)
$2.47 \pm 0.1\%$	$0.54 \pm 2.0\%$ (78)	$295 \pm 0.9\%$ (531)	$53.8 \pm 0.9\%$ (16.3)
$2.95 \pm 0.3\%$	$0.76 \pm 2.7\%$ (110)	$295 \pm 0.9\%$ (531)	$58.9 \pm 1.9\%$ (17.8)
$3.44 \pm 0.2\%$	$1.03 \pm 3.0\%$ (150)	$295 \pm 0.8\%$ (531)	$64.0 \pm 1.7\%$ (19.4)
$3.95 \pm 0.4\%$	$1.58 \pm 5.0\%$ (230)	$295 \pm 1.3\%$ (531)	$75.8 \pm 1.7\%$ (23.0)

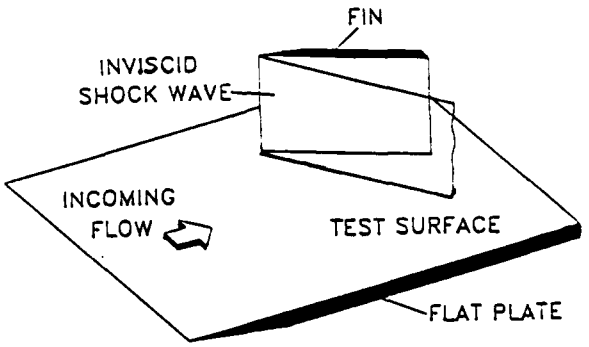

Figure 1: Test model.

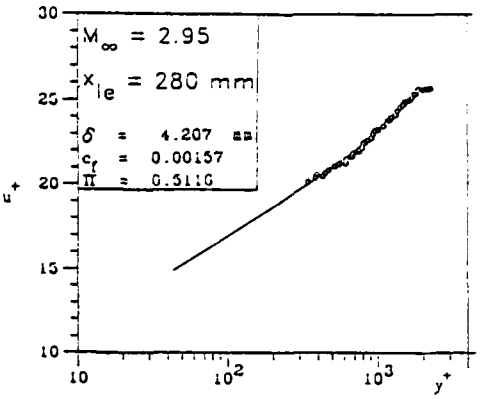

Figure 3: Undisturbed boundary-layer profile.

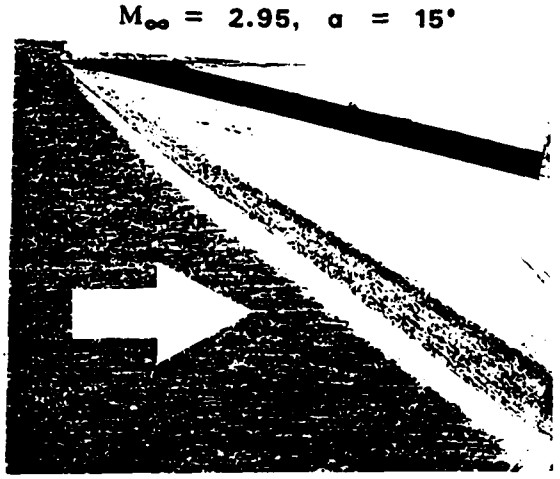

a. Example.

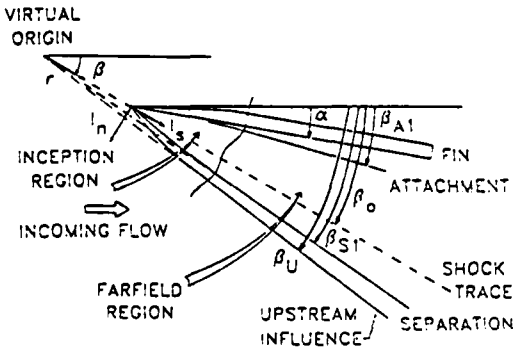

b. Sketch showing key surface features.

Figure 2: Surface-flow visualization results.

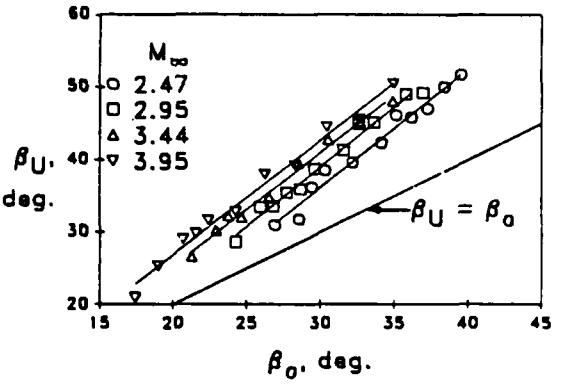

Figure 4: The effects of M_∞ and β_o on β_U.

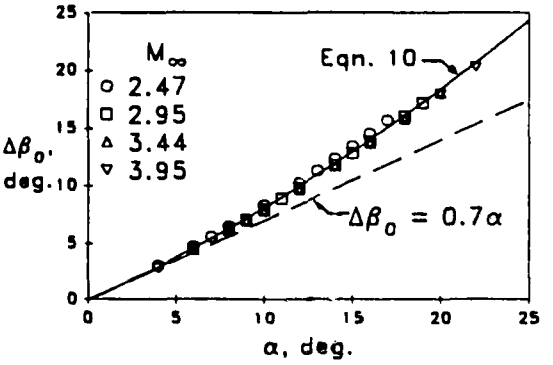

Figure 5: The nonlinear growth of $\Delta\beta_o$ with α.

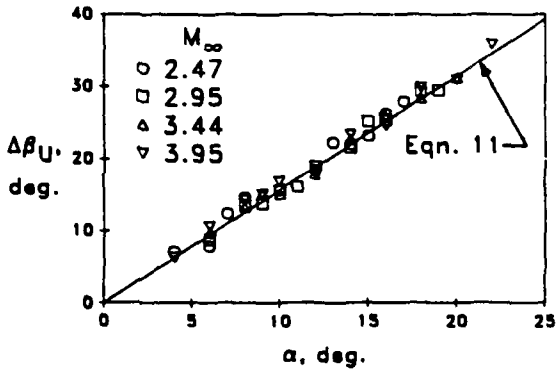

Figure 6: The linear growth of $\Delta\beta_U$ with α.

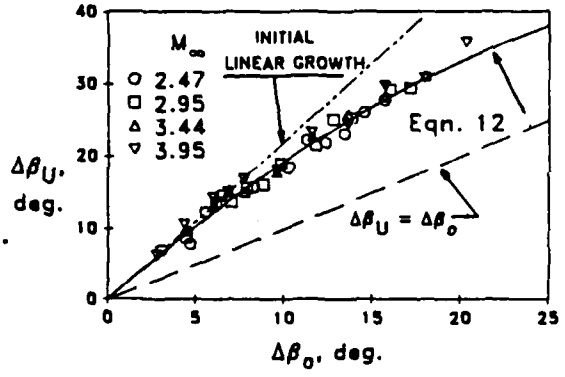

Figure 7: Scaling of $\Delta\beta_U$ by $\Delta\beta_0$.

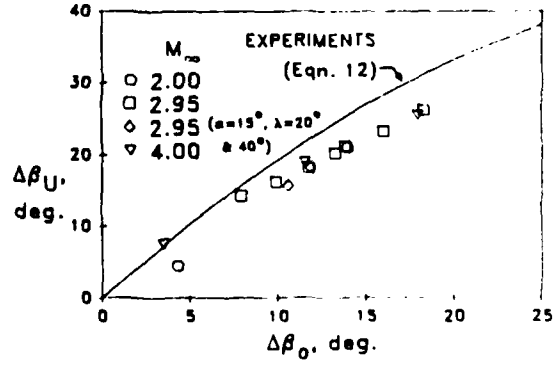

Figure 8: Scaling of computed $\Delta\beta_U$ by $\Delta\beta_0$.

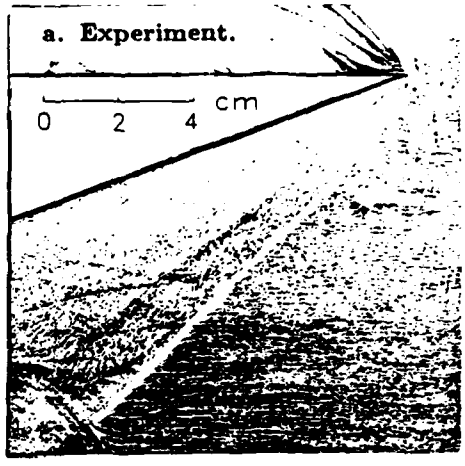

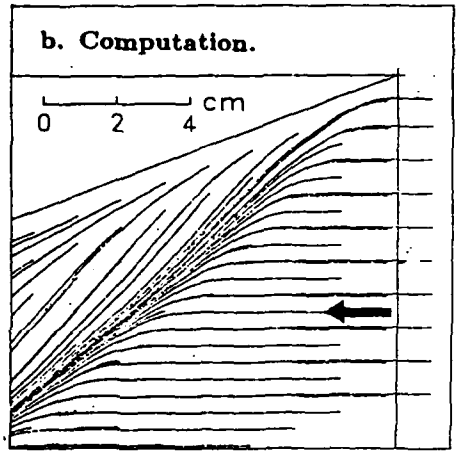

Figure 9: Comparison between experimental surface-flow visualization and computed skin-friction lines ($M_\infty = 4$, $\alpha = 20°$).

END

FEb.

1988

DTIC